

Decoherence Control by Tracking a Hamiltonian Reference Molecule

Gil Katz,¹ Mark A. Ratner,¹ and Ronnie Kosloff²

¹*Department of Chemistry, Northwestern University, Evanston, Illinois 60208-3113, USA*

²*Fritz Haber Research Center for Molecular Dynamics, Hebrew University of Jerusalem, Jerusalem, 91904, Israel*
(Received 10 February 2006; revised manuscript received 15 February 2007; published 17 May 2007)

A molecular system in contact with a bath undergoes strong decoherence processes. We examine a control scheme to minimize dissipation, while maximally retaining coherent evolution, by relating the evolution of the molecule to that of an identical freely propagating system. We seek a driving field that maximizes the projection of the open molecular system onto the freely propagated one. The evolution in time of a molecular system consisting of two nonadiabatically coupled electronic states interacting with a bath is followed. The driving control field that overcomes the decoherence is calculated. A proposition to implement the scheme in the laboratory using feedback control is suggested.

DOI: 10.1103/PhysRevLett.98.203006

PACS numbers: 33.80.Ps, 02.30.Yy, 82.50.Nd, 82.53.Kp

Coherent control originated as a method to steer a chemical reaction to a desired outcome [1–3]. The usual agent of control is quantum interference [4]. The purpose of the endeavor is to find means, usually through shaping an electromagnetic field (EM), to direct the process to its target. In condensed phases coherent evolution is degraded by dissipative forces in the environment, termed decoherences. Since generation of interference pathways is a global process in time, an intervention at one instant influences the subsequent evolution and can interfere at later times with another intervention. To address this issue optimal control theory (OCT) has been developed as a mathematical tool common in various engineering fields [5] that searches forward and backwards iteratively for the optimal pulse [6,7].

Local control theory (LCT) is a unidirectional time propagation scheme to determine the instantaneous phase of the EM field that monotonically increases the expectation of a target operator [8–10]. Although OCT can lead to superior results, LCT has the advantage that the control mechanism can be interpreted, and the iterative time propagation procedure is absent. Tracking control originated from the idea of changing the local field in order to follow a reference state [11–14]. Tracking can be considered as local control with a time dependent target. This tracking mechanism differs from OCT since it follows the reaction path rather than optimizing backward from a chosen outcome [15].

Our basic idea here is to use a freely propagating molecule as a tracking target for an identical molecule in a dissipative environment. The perfect tracking field will then null the dissipative forces and protect the molecule from decoherence. The question to be addressed is how can an external field that generates a unitary transformation protect the system against nonunitary dissipative forces? A computational model of an online dynamic decoherence control method is explored. The method is established by simultaneously following the evolution in time of a system with and without the bath, thus using the overlap between the two systems to construct a correcting electric field

which is directly applied back on the system. The method is explored for the fastest dissipative mechanism, environment-induced electronic quenching from an excited state to a lower state (the approximate decay time in solid state systems is less than 50 fsec). The coherence time of the system is extended by an order of magnitude using the simplest tracking method.

Measuring the overlap between the controlled and the target system also underlies a proposed experimental approach. This observable can then be employed as a basis for a learning loop used to optimize a control field.

The molecular system is described by the density operator $\hat{\rho}$, a function of nuclear and electronic degrees of freedom. The reference or target system $\hat{\rho}_{\text{tar}}$ evolves freely under its Hamiltonian $\hat{\mathbf{H}}_0$:

$$\dot{\hat{\rho}}_{\text{tar}} = -i[\hat{\mathbf{H}}_0, \hat{\rho}_{\text{tar}}], \quad (1)$$

where $\hbar \equiv 1$ is chosen. The subjected system $\hat{\rho}_S$ is coupled to a bath: $\hat{\rho}_S = \text{Tr}_B\{\hat{\rho}_{SB}\}$. This evolves according to:

$$\dot{\hat{\rho}}_{SB} = -i[\hat{\mathbf{H}}_T, \hat{\rho}_{SB}], \quad (2)$$

where $\hat{\rho}_{SB}$ is the combined system-bath operator. The dynamics is generated by the combined system-bath Hamiltonian $\hat{\mathbf{H}}_T = \hat{\mathbf{H}}_0 + \hat{\mathbf{H}}_B + \hat{\mathbf{H}}_{SB}$. The first approach employed to solve the open system dynamics is based on renormalized bath operators $\hat{\mathbf{H}}_B + \hat{\mathbf{H}}_{SB}$ represented explicitly. The equations of motion are solved in a larger Hilbert space (the surrogate Hamiltonian method [16]). The system density operator is obtained from $\hat{\rho}_S = \text{Tr}_B\{\hat{\rho}_{SB}\}$.

In the second approach, based on the Markovian limit, the reduced dynamics of the open quantum system $\hat{\rho}_S$ [17] can be described by the generator $\dot{\hat{\rho}}_S = -i[\hat{\mathbf{H}}_0, \hat{\rho}_S] + \mathcal{L}_D(\hat{\rho}_S)$, where \mathcal{L}_D describes the bath-induced decoherence dynamics, conveniently cast into the Lindblad semi-group form:

$$\mathcal{L}_D(\hat{\rho}_S) = \sum_j (\hat{\mathbf{F}}_j \hat{\rho}_S \hat{\mathbf{F}}_j^\dagger - \frac{1}{2}(\hat{\mathbf{F}}_j^\dagger \hat{\mathbf{F}}_j, \hat{\rho}_S)), \quad (3)$$

where $\{\hat{\mathbf{A}}, \hat{\mathbf{B}}\} = \hat{\mathbf{A}}\hat{\mathbf{B}} + \hat{\mathbf{B}}\hat{\mathbf{A}}$ is the anticommutator and $\hat{\mathbf{F}}$ are operators from the Hilbert space of the system. The nature of the bath interaction determines the form of the Lindblad operators $\hat{\mathbf{F}}$. The choice of $\hat{\mathbf{F}}$ determines the dissipative model considered.

Our purpose is to control the system coupled to the bath and force it to follow as closely as possible the dynamics of the freely evolving reference system, $\hat{\rho}_{\text{tar}}$. The external control field $\epsilon(t)$ is coupled to the system through the transition dipole of the molecule. The control Hamiltonian becomes $\hat{\mathbf{H}}_c = \hat{\boldsymbol{\mu}}\epsilon(t)$ leading to the a combined dynamics of the controlled system $\hat{\rho}_C$ generated by: $\hat{\mathbf{H}}_T = \hat{\mathbf{H}}_0 + \hat{\mathbf{H}}_B + \hat{\mathbf{H}}_{SB} + \hat{\mathbf{H}}_c$.

The challenge of decoherence control is to find the field, $\epsilon(t)$, that induces the dynamics of the system $\hat{\rho}_C(t)$ to be as close as possible to $\hat{\rho}_{\text{tar}}$. This is attacked by maximizing the overlap functional $J(t)$ between the target and controlled states:

$$J(t) = (\hat{\rho}_C \cdot \hat{\rho}_{\text{tar}}) \equiv \text{Tr}\{\hat{\rho}_C \hat{\rho}_{\text{tar}}\} = \langle \hat{\rho}_{\text{tar}} \rangle. \quad (4)$$

$J(t)$ can be interpreted as the expectation of the target density operator in the controlled state. To achieve this target the control field should increase the expectation of the target operator. The Heisenberg equation of motion for the observable $\langle \hat{\rho}_{\text{tar}} \rangle$ generated by the control Hamiltonian becomes:

$$\frac{d}{dt} \langle \hat{\rho}_{\text{tar}} \rangle = -i \langle [\hat{\mathbf{H}}_c, \hat{\rho}_{\text{tar}}] \rangle = \quad (5)$$

$$-i \epsilon(t) \text{Tr}\{\hat{\boldsymbol{\mu}} \hat{\rho}_{\text{tar}} \hat{\rho}_C - \hat{\rho}_{\text{tar}} \hat{\boldsymbol{\mu}} \hat{\rho}_C\}. \quad (6)$$

The control field is constructed by requiring maximal $J(t)$, so that $\frac{d}{dt} \langle \hat{\rho}_{\text{tar}} \rangle \geq 0$ at any instant, leading to:

$$\epsilon(t) = -iK \text{Tr}\{\hat{\rho}_C \hat{\boldsymbol{\mu}} \hat{\rho}_{\text{tar}} - \hat{\rho}_{\text{tar}} \hat{\boldsymbol{\mu}} \hat{\rho}_C\}^*, \quad (7)$$

where $K = K(t)$ is a positive envelope function with dimension $\frac{\text{energy}}{(\text{dipole})^2}$. From Eq. (7) it is clear that the correcting field $\epsilon(t) = 0$ if $\hat{\rho}_C$ approaches $\hat{\rho}_{\text{tar}}$.

We adopt a molecular model system with two electronic states described by the density operator:

$$\hat{\rho} = \begin{pmatrix} \hat{\rho}_e & \hat{\rho}_{eg} \\ \hat{\rho}_{ge} & \hat{\rho}_g \end{pmatrix}, \quad (8)$$

where the indices g and e designate the ground and excited electronic states and the submatrices are functions of the nuclear coordinates. The Hamiltonian of the system has the form:

$$\hat{\mathbf{H}}_0 = \begin{pmatrix} \hat{\mathbf{H}}_e & \hat{\mathbf{V}}_{eg} \\ \hat{\mathbf{V}}_{ge} & \hat{\mathbf{H}}_g \end{pmatrix} \quad (9)$$

with $\hat{\mathbf{H}}_{g/e} = \hat{\mathbf{T}} + \hat{\mathbf{V}}_{g/e}$. $\hat{\mathbf{T}}$ is the kinetic energy operator, $\hat{\mathbf{V}}_g$ and $\hat{\mathbf{V}}_e$ are the potential energy operators on the ground and excited electronic states, and $\hat{\mathbf{V}}_{eg}$ is the nonadiabatic coupling potential. The control Hamiltonian is chosen as:

$$\hat{\mathbf{H}}_c = \begin{pmatrix} 0 & -\hat{\boldsymbol{\mu}}^\dagger \epsilon(t) \\ -\hat{\boldsymbol{\mu}} \epsilon(t) & 0 \end{pmatrix}, \quad (10)$$

where $\hat{\boldsymbol{\mu}}$ is the coordinate dependent electronic transition dipole element. The dissipation phenomena included in the model were fast electronic quenching, vibrational, and electronic dephasing. $\hat{\mathbf{F}}_q = \sqrt{\gamma_q}(|e\rangle\langle g|)$ is chosen to model fast electronic quenching. The choice $\hat{\mathbf{F}}_{\text{vd}} = \frac{\sqrt{\gamma_{\text{vd}}\phi}}{\hbar} \hat{\mathbf{H}}_{\text{vd}}$ dictates pure vibrational dephasing of the system. $\hat{\mathbf{F}}_{\text{ed}} = \sqrt{\gamma_{\text{ed}}}(|e\rangle\langle e| - |g\rangle\langle g|)$ represents electronic dephasing [16]. These choices of system/bath interaction terms will lead to processes with a characteristic dissipation rates γ_y . The dominant term would be the fast electronic quenching rate.

The control field form Eq. (7) becomes:

$$\begin{aligned} \epsilon(t) = & K \text{Im}(\text{Tr}_Q\{\hat{\rho}_c^{ge} \hat{\boldsymbol{\mu}} \hat{\rho}_{\text{tar}}^{ge}\} + \text{Tr}_Q\{\hat{\rho}_c^e \hat{\boldsymbol{\mu}} \hat{\rho}_{\text{tar}}^{ge}\} \\ & - \text{Tr}_Q\{\hat{\rho}_{\text{tar}}^{ge} \hat{\boldsymbol{\mu}} \hat{\rho}_c^{ge}\} - \text{Tr}_Q\{\hat{\rho}_{\text{tar}}^e \hat{\boldsymbol{\mu}} \hat{\rho}_c^{ge}\} \\ & - \text{Tr}_Q\{\hat{\rho}_{\text{tar}}^{ge} \hat{\boldsymbol{\mu}} \hat{\rho}_c^{eg}\} + \text{Tr}_Q\{\hat{\rho}_c^{ge} \hat{\boldsymbol{\mu}} \hat{\rho}_{\text{tar}}^{eg}\} \\ & - \text{Tr}_Q\{\hat{\rho}_{\text{tar}}^{eg} \hat{\boldsymbol{\mu}} \hat{\rho}_c^{ge}\} + \text{Tr}_Q\{\hat{\rho}_c^{eg} \hat{\boldsymbol{\mu}} \hat{\rho}_{\text{tar}}^{ge}\}), \end{aligned} \quad (11)$$

where Tr_Q is a partial trace over the coordinates.

The computational model is constructed from two electronic states of a diatomic molecule represented by two diabatic Morse potential energy surfaces. Using dimensionless normal coordinates:

$$\begin{aligned} V_g(\hat{\mathbf{Q}}) &= -\Delta + D_g(1 - \exp[-a_g(\hat{\mathbf{Q}} - Q_g)^2]), \\ V_e(\hat{\mathbf{Q}}_0) &= \Delta + D_e(1 - \exp[-a_e(\hat{\mathbf{Q}} - Q_e)^2]), \end{aligned} \quad (12)$$

where D_g and D_e are the dissociation energies of the ground and excited electronic states, 2Δ is the adiabatic excitation energy, and a is the width of the state. Q_e and Q_g are the equilibrium bond lengths of the two electronic states. ($D_g = D_e = 1.25$ eV, $\Delta = 0.3$ eV, $a_e = 0.8 \text{ \AA}^{-2}$, $a_g = 1.5 \text{ \AA}^{-2}$, $V_{ge/eg} = 0.05$ eV, $Q_g = 0 \text{ \AA}$, $Q_e = 0.1 \text{ \AA}$, and $\hat{\boldsymbol{\mu}} = 1.0$.)

The time evolution was obtained by solving either the non-Markovian Surrogate Hamiltonian method or the semigroup time dependent Liouville-von Neumann equation. A grid was used for the spatial coordinates and time propagation used the Chebychev scheme [18]. The initial ground vibronic state of the system was calculated via a relaxation scheme [19]. A pump pulse transfers a significant fraction of the population from the ground to the excited electronic state. A Gaussian form is chosen for this pulse:

$$\epsilon_{\text{pump}}(t) = \epsilon_0 e^{-(t-t_{\text{max}})^2/2\sigma_L^2} e^{i\omega_L t}. \quad (13)$$

The carrier frequency ω_L is chosen to match the difference between the ground and excited electronic potentials at the minimum of the ground state $Q = 0$. The width of the pulse σ_L was adjusted to a FWHM duration of 12 fsec and the amplitude $\epsilon_0 \mu = 0.228$ eV.

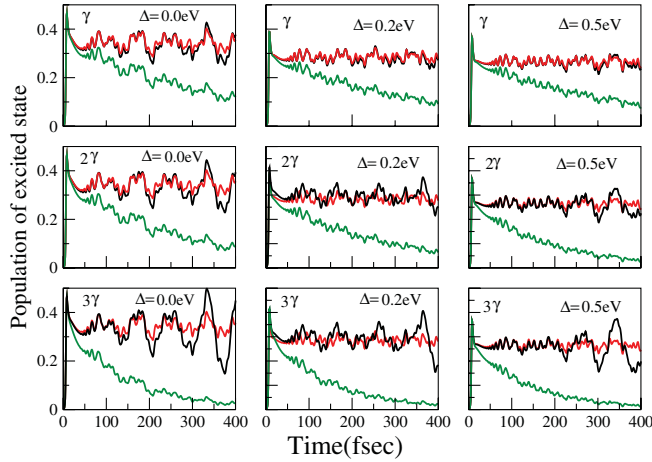


FIG. 1 (color). The population of the excited state as a function of time for the target state $\hat{\rho}_{\text{tar}}$ (red), the controlled density operator $\hat{\rho}_C$ (black), and the uncontrolled system density operator $\hat{\rho}_S$ (green) for different magnitudes of quenching (columns) and Δ 's (rows). $\gamma = 0.003 \text{ fsec}^{-1}$.

At this point three parallel propagations of the density operator were performed. The first for $\hat{\rho}_{\text{tar}}$ was carried out only with the Hamiltonian term Eq. (1). The system density operator, $\hat{\rho}_S$, was propagated with the dissipative \mathcal{L}_D included, Eq. (2). The controlled density operator, $\hat{\rho}_C$, was propagated with both the dissipative \mathcal{L}_D and the correcting field applied terms. The correction field was calculated according to Eq. (11) at each time step and fed back in the next time step. Both Markovian and non-Markovian methods gave similar results.

The systems free dynamics represents a complex population oscillation between the two electronic states. The excited state population is shown in Fig. 1 for the controlled $\hat{\rho}_C$, uncontrolled $\hat{\rho}_S$, and target $\hat{\rho}_{\text{tar}}$ for different quenching parameters γ and energy gap Δ . In all cases a fast decay of the excited state is seen for the uncontrolled state. The controlled state is able to track the target state and maintain the population. When the quenching increases the controlled system is still able to follow the overall dynamics of the target but not the finer details. As can be seen in Fig. 1, the control ability increases with the energy gap Δ . The control field ϵ is shown in Fig. 2 in time and frequency. In general the field is composed of a central frequency corresponding to the energy gap modulated by the vibrational frequency. The actual vibronic lines are missing from the spectrum [20]. Wigner plots (not shown) show phase locking between the frequency components.

The changes in purity $\text{Tr}\{\hat{\rho}^2\}$ and in the scalar product with the target state ($\hat{\rho} \cdot \hat{\rho}_{\text{tar}}$) show a different viewpoint on the decoherence control cf. Fig. 3. The uncontrolled state $\hat{\rho}_S$ undergoes fast exponential decay of both measures in time. The controlled purity $\text{Tr}\{\hat{\rho}_C^2\}$ maintains a high value as does the scalar product ($\hat{\rho}_C \cdot \hat{\rho}_{\text{tar}}$). The general trend is a

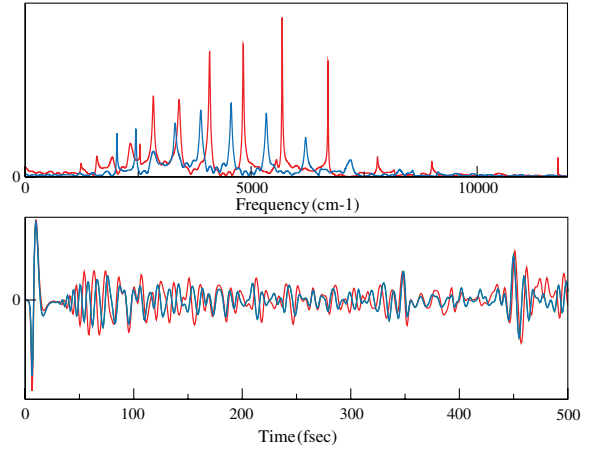


FIG. 2 (color). Typical control field in frequency (top left) and time domain (bottom) for $\gamma = 0.003$ (blue) and $\gamma = 0.006 \text{ fsec}^{-1}$ (red).

linear decay in time. The oscillations around this decay and the local increase in purity suggest that a cooling mechanism is taking place [20]. To gain insight on this possibility the correcting field was stopped for 100 fsec and resumed again, Fig. 4. As expected, once the control field is turned off the purity and the scalar product of the controlled state $\hat{\rho}_C$ decrease sharply. When the controlling field is resumed an almost linear increase in both parameters can be observed. Such an effect can only be the result of a cooling mechanism which represents an interplay between the nonunitary dissipation and the unitary control field [20]. It is clear [21] that simple unitary transformation cannot induce cooling.

The present results show that the decoherence can be suppressed, extending good overlap with the target by an order of magnitude in time. The model calculation establishes the principle that a correcting external field can be found which protects the system from decoherence. Here

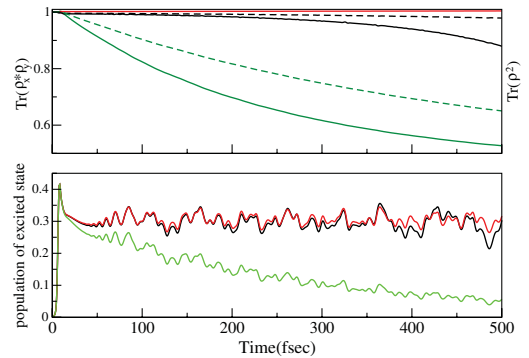


FIG. 3 (color). Top: the purity $\text{Tr}\{\hat{\rho}^2\}$ (solid line) and the scalar product with the target state ($\hat{\rho} \cdot \hat{\rho}_{\text{tar}}$) (dashed line) for the target state $\hat{\rho}_{\text{tar}}$ (red) the controlled density operator $\hat{\rho}_C$ (black) and the reference uncontrolled density operator $\hat{\rho}_S$ (green). Bottom: the population of the excited state, same color codes.

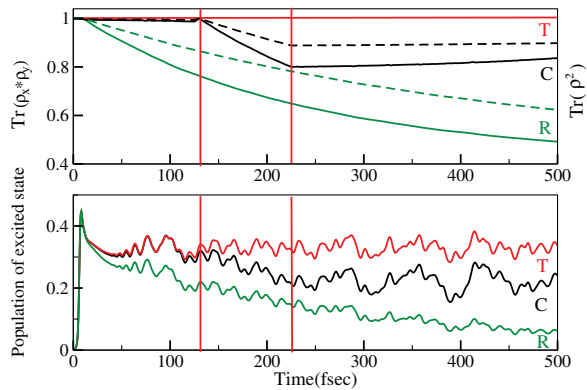


FIG. 4 (color). Turning off the control field. Top: the purity $\text{Tr}\{\hat{\rho}^2\}$ (solid line) and the scalar product with the target state ($\hat{\rho} \cdot \hat{\rho}_{\text{tar}}$) (dashed line) for the target state $\hat{\rho}_{\text{tar}}$ (red), the controlled density operator $\hat{\rho}_C$ (black), and the reference uncontrolled density operator $\hat{\rho}_S$ (green). The vertical lines indicate the time interval where the control field is turned off. Bottom: the population of the excited state as a function of time, same color codes.

we discuss control to overcome fast electronic dephasing; while the rapid modulations in Fig. 2 are not currently attainable, the essential behavior is correct.

The nearly complete distinction between coherent (gas) and decoherent (condensed) phase molecular dynamics has decreased with the evolution of nanoscale science. It is easy to imagine applications that require preservation of the decoherence-free properties of a system upon becoming a subsystem of a larger apparatus. This ability may have significant importance in many future applications, for example, extending lifetime of the read or write process in quantum information processing, or memory chips and switches in molecular electronics. One might even imagine implementations for localizing intramolecular gas phase properties to a specific part or chemical bond of a macromolecule. Thus retaining a level of decoherence-free behavior in a given subspace is a significant goal. The scheme suggested allows a driving process to control such decoherence and to retain coherent evolution in the subspace.

The proof of principle then shifts attention to finding such a field in the laboratory. The idea is to use an actual freely evolving molecule as the target for an identical molecule subject to a dissipative environment such as in solution or on a surface. The correcting feedback should be set such that the difference in transient absorption of the two molecules is minimized.

To implement the present scheme in the laboratory the key element is to apply a scalar product between the states of the reference and controlled systems: ($\hat{\rho}_C \cdot \hat{\rho}_{\text{tar}}$) (displayed in Fig. 3). To make this task possible the two isolated states should become part of the same quantum system. This can be carried out by placing the controlled system $\hat{\rho}_C$ and the reference system $\hat{\rho}_{\text{tar}}$ in two branches of

an interferometer [22]. A pair of twin ultrashort photons which can be created by down conversion are split spatially. Then they are directed to the two branches of the interferometer interrogating the two systems. The transmitted photons are then redirected to interfere with each other. Any difference between the target and the controlled system will degrade this interference. The interference signal can then be used as a feedback to generate the correcting field [23].

We are grateful to the BSF and the NSF chemistry division for support of this work.

- [1] D. Tannor and S. Rice, *J. Chem. Phys.* **83**, 5013 (1985).
- [2] D. J. Tannor, R. Kosloff, and S. Rice, *J. Chem. Phys.* **85**, 5805 (1986).
- [3] P. Brumer and M. Shapiro, *Acc. Chem. Res.* **22**, 407 (1989).
- [4] R. Gordon and S. Rice, *Annu. Rev. Phys. Chem.* **48**, 601 (1997).
- [5] A. Bryson and Y. Ho, *Applied Optimal Control* (Hemisphere, New York, 1975).
- [6] W. S. Warren, H. Rabitz, and M. Dahleh, *Science* **259**, 1581 (1993).
- [7] R. Kosloff, S. A. Rice, P. Gaspard, S. Tregiani, and D. J. Tannor, *Chem. Phys.* **139**, 201 (1989).
- [8] R. Kosloff, A. D. Hammerich, and D. J. Tannor, *Phys. Rev. Lett.* **69**, 2172 (1992).
- [9] A. Bartana, R. Kosloff, and D. J. Tannor, *J. Chem. Phys.* **99**, 196 (1993).
- [10] F. L. Yip, D. A. Mazziotti, and H. Rabitz, *J. Phys. Chem. A* **107**, 7264 (2003).
- [11] W. Zhu, M. Smit, and H. Rabitz, *J. Chem. Phys.* **110**, 1905 (1999).
- [12] W. Zhu and H. Rabitz, *J. Chem. Phys.* **119**, 3619 (2003).
- [13] M. Guhr and N. Schwentner, *Phys. Chem. Chem. Phys.* **7**, 760 (2005).
- [14] M. Guhr, H. Ibrahim, and N. Schwentner, *Phys. Chem. Chem. Phys.* **6**, 5353 (2004).
- [15] S. Kallush and R. Kosloff, *Phys. Rev. A* **73**, 032324 (2006).
- [16] D. Gelman, G. Katz, R. Kosloff, and M. A. Ratner, *J. Chem. Phys.* **123**, 134112 (2005).
- [17] G. Lindblad, *Commun. Math. Phys.* **48**, 119 (1976).
- [18] W. Huisinga, L. Pesce, R. Kosloff, and P. Saalfrank, *J. Chem. Phys.* **110**, 5538 (1999).
- [19] R. Kosloff and H. Tal-Ezer, *Chem. Phys. Lett.* **127**, 223 (1986).
- [20] A. Bartana, R. Kosloff, and D. J. Tannor, *Chem. Phys.* **267**, 195 (2001).
- [21] W. Ketterle and D. Pritchard, *Phys. Rev. A* **46**, 4051 (1992).
- [22] B. Dayan, A. Pe'er, A. A. Friesman, and Y. Silberberg, *Phys. Rev. Lett.* **94**, 043602 (2005).
- [23] D. A. Steck, K. Jacobs, H. Mabuchi, T. Bhattacharya, and S. Habib, *Phys. Rev. Lett.* **92**, 223004 (2004).